^2S Rydberg spectrum of the boron atom

István Hornyák,[1,*] Saeed Nasiri,[1,†] Sergiy Bubin,[1,‡] and Ludwik Adamowicz[2,3,4,§]

[1]*Department of Physics, Nazarbayev University, Nur-Sultan 010000, Kazakhstan*

[2]*Department of Chemistry and Biochemistry, University of Arizona, Tucson, Arizona 85721, USA*

[3]*Department of Physics, University of Arizona, Tucson, Arizona 85721, USA*

[4]*Interdisciplinary Center for Modern Technologies, Nicolaus Copernicus University, ulica Wileńska 4, Toruń PL 87-100, Poland*

(Received 9 June 2021; accepted 23 August 2021; published 8 September 2021)

Benchmark variational calculations of the lowest ten Rydberg ^2S states of two stable isotopes of the boron atom (^{10}B and ^{11}B) are reported. The nonrelativistic wave functions of this five-electron system are expanded in terms of 16 000 all-particle explicitly correlated Gaussians (ECGs). The ECG nonlinear exponential parameters are extensively optimized using a procedure that employs the analytic gradient of the energy with respect to these parameters. A finite nuclear mass value is used in the calculations and the motion of the nucleus is explicitly represented in the nonrelativistic Hamiltonian. The leading relativistic corrections to the energy levels are computed in the framework of the perturbation theory. The lowest-order quantum electrodynamics corrections are also estimated. The results obtained for the energy levels enable determination of interstate transition frequencies with accuracy that approaches the available experimental spectroscopic data.

DOI: 10.1103/PhysRevA.104.032809

I. INTRODUCTION

Expanding an atomic wave function in terms of explicitly correlated basis functions that depend on the interelectron distances can yield a highly accurate representation of the atomic system provided the basis functions are thoroughly optimized. For example, employing explicitly correlated basis functions, the nonrelativistic energies of the He atom were determined with accuracy that exceeds 20 and, in some studies, even 40 digits [1–6]. For the lithium atom, accuracy of up to 15 digits has been achieved [7–10].

The He and Li calculations were done with the use of Hylleraas basis functions that properly describe the behavior of the wave function at the atomic nucleus as well as a finite distance from the nucleus [10–12]. The application of the Hylleraas basis functions in calculations of energy levels of atoms with more electrons has been difficult due to complications with calculating the Hamiltonian matrix elements with these functions. Thus, only limited cases of four-electron systems have been considered [13,14].

An alternative to using Hylleraas basis functions in atomic calculations is to use all-electron explicitly correlated Gaussian (ECGs) functions [15–23]. The ECGs depend exponentially on the squares of the interelectron distances and, thus, they do not strictly satisfy the Kato's cusp conditions. This deficiency can be effectively remediated by using a large number of basis functions and by performing extensive optimization of their nonlinear exponential parameters [24,25] as it is done in the present work. Employing ECGs in the calculations enables accurate description of the electron correlation effects, which is key in high-precision calculations of atomic spectra. These effects are related to the electrostatic repulsion between the electrons and their avoiding each other in their motion around the nucleus. Effective atomic basis functions should be capable to accurately describe the decrease of the probability of two or more electrons being found close to each other (see the section on the basis functions used in the present work for more discussion on this matter).

The variational optimization of the ECG exponential parameters is carried out with the use of analytically calculated first derivatives of the energy determined with respect to the parameters. These derivatives form the energy gradient vector, which is supplied to the subroutine that runs the variational energy minimization. The use of the gradient significantly accelerates the energy convergence of the calculation. As shown in this work on the boron excited ^2S spectrum, it also allows to consider a relatively large set of the Rydberg states of an atom. The use of the energy gradient in the present calculations, which is unique to our approach, resembles the use of the energy gradient in the calculation of an equilibrium molecular geometry performed using orbital Gaussians with centers placed at the nuclei of the atoms forming the molecule. Also there, the analytically calculated energy derivatives determined with respect to the coordinates of the nuclei of the atoms forming the molecule are used to find the molecular geometry that corresponds to an energy minimum. As the Gaussian centers in the calculation coincide with the atomic centers, the analytical derivatives of the energy expression with respect to the molecular geometrical parameters are expressed in terms of the derivatives of the Hamiltonian and

*Present address: Institute of Chemistry, ELTE Eötvös Loránd University, Pázmány Péter sétány 1/A, 1117 Budapest, Hungary; ihornyak@caesar.elte.hu

†saeed.nasiri@nu.edu.kz

‡sergiy.bubin@nu.edu.kz

§ludwik@arizona.edu

overlap matrix elements determined with respect to these parameters. This is similar to the approach used in this work where the derivatives are also calculated with respect to the parameters of the Gaussians. However, in the present work these parameters are not the coordinates of the Gaussian centers but the exponential parameters [e.g., parameters α_1, α_2, and β in Eq. (4)].

With increasing capabilities of present-day computers, the frontier of very accurate calculations of atomic spectra is shifting from four-electron systems to systems with five electrons. The boron atom and five-electron atomic ions become targets of the investigation. In the present work, ten lowest ^2S states of ^{10}B and ^{11}B, as well as of $^{\infty}$B, are calculated using extended sets of the ECG basis functions. The calculations include the leading relativistic and quantum-electrodynamics (QED) energy corrections. The algorithms for calculating these corrections include integrals that are more intricate than the integrals involved in the overlap and Hamiltonian matrix elements and the matrix elements of the analytical energy gradient. Also, the relativistic and QED matrix elements are more sensitive to imperfections of the Gaussian used for expanding the wave function. These imperfections include improper asymptotic behavior of the ECGs decaying too fast at long distances and their inadequate short-range behavior of not correctly describing the Kato's cusp conditions. These drawbacks can, however, be partially overcome by applying the so-called "regularization" techniques and using large well-optimized basis sets (see the next section).

One of the motivating factors for carrying out the present calculations is the realization that a much higher accuracy can now be achieve in boron calculations with the use of the gradient-aided optimization of the ECG exponential parameters. For example, the best previous calculations of the lowest ^2S state of $^{\infty}$B performed by Puchalski *et al.* [26] using 8192 ECGs resulted in the nonrelativistic variational energy of -24.471393366 hartree. As one will see in the Results section, the present $^{\infty}$B energy value of -24.471393641 hartree obtained with 16 000 ECGs is noticeably lower. Also, our energy is close to the asymptotic estimate of a complete-basis-set energy value of $-24.47139368(32)$ hartree given by Puchalski *et al.* [26].

Finally, it should be mentioned that atomic calculations performed with all-electron ECGs are very time consuming. The bottleneck is the very steep dependency of the calculation time on the number of electrons in the system which, is $n!$. This number is equal to the number of operators representing the electron-label permutations that need to be applied to each ECG to implement the proper permutational symmetry of the wave function. $n!$ is also equal to the number of elemental integrals that need to be calculated to determine the value of a single Hamiltonian matrix element or a matrix element of any other operator used in the present calculations, e.g., the operators representing the leading relativistic effects. So, even though the calculations of the matrix elements can be very efficiently parallelized in the calculation, the large number of the integrals calculated in each step of the basis set optimization makes the calculation very expensive. At present, very accurate ECG atomic calculations are practically limited to systems with five or less electrons. The present work is an example of such calculations. Even though we have written codes to perform ECG calculations for carbon and nitrogen atoms [27,28], more powerful computers will be needed to take full advantage of these codes.

II. THE METHOD

A. Nonrelativistic nuclear-mass-dependent Hamiltonian

Very accurate atomic calculations have to account for the effects associated with the finite mass of a nucleus. This can be done using the perturbation-theory approach (most common way) or more explicitly by including these effects in the Hamiltonian that represents the nonrelativistic energy of the system. In the present work, the latter approach is used. The finite-nuclear-mass (FNM) effects are revealed when the internal motion of the atom is considered as a coupled motion of the nucleus and the electrons around the center of mass of the system. Thus, to calculate the energies and the corresponding wave functions of bound states associated with this motion, an internal atomic nonrelativistic Hamiltonian has to be derived. In the approach used here, the starting point in the derivation of such a Hamiltonian is the standard nonrelativistic laboratory-frame Hamiltonian comprising operators representing the kinetic and potential energies of the nucleus and the electrons. The laboratory-frame Hamiltonian is expressed in terms of the Cartesian laboratory-frame coordinates. Next, a new coordinate system is introduced consisting of the three coordinates, X_{CM}, Y_{CM}, and Z_{CM}, that represent the position of the center of mass of the atom in the laboratory frame and $3N-3=3n$ internal coordinates, where N is the total number of particles in the atom, i.e., the number of electrons, n, plus one. There are a number of ways the internal coordinates can be chosen. In the present approach we use a generalization of the textbook approach employed in solving the Schrödinger equation for the hydrogen atom, where the internal coordinates are the coordinates of the vector with the origin at the proton and the end at the electron. Thus, in the generalized approach used here, the internal coordinates are the coordinates of the vectors $\mathbf{r}_i$, $i=1,\ldots,n$, originating at the nucleus and ending at the individual electrons. Now, when the laboratory-frame Hamiltonian is expressed in terms of the new coordinates, it rigorously splits into an operator representing the kinetic energy of the motion of the center of mass and an operator dependent only on the internal coordinates that represents the internal state of the system [29]. The internal Hamiltonian has the following form:

$$H_{\rm nr}^{\rm int} = -\frac{1}{2}\left(\sum_{i=1}^{n}\frac{1}{\mu_i}\nabla_{\mathbf{r}_i}^2 + \sum_{i=1}^{n}\sum_{j\neq i}^{n}\frac{1}{m_0}\nabla'_{\mathbf{r}_i}\nabla_{\mathbf{r}_j}\right) + \sum_{i=1}^{n}\frac{q_0 q_i}{\mathbf{r}_i} + \sum_{i=1}^{n}\sum_{j<i}^{n}\frac{q_i q_j}{\mathbf{r}_{ij}}, \tag{1}$$

where q_0 is the charge of the nucleus, $q_i=-1$ $(i=1,\ldots,n)$ are the electron charges, m_0 is the nuclear mass, $\mu_i = m_0 m_i/(m_0+m_i)$ is the reduced mass of electron i ($m_i = m_e = 1$), and $r_{ij}=|\mathbf{r}_j-\mathbf{r}_i|$ is the distance between electrons i and j. In this work we adopted the following values of the nuclear masses: $m_0(^{10}\mathrm{B}) = 18247.46879 m_e$ and $m_0(^{11}\mathrm{B}) = 20063.73729 m_e$, where m_e is the mass of the electron.

These nuclear masses can be obtained from the experimentally derived atomic masses, 10.012936862(16) u and 11.009305167(13) u, respectively [30], by subtracting the masses of five bound electrons and adding the total electron binding energy. The infinite-nuclear-mass (INM) Hamiltonian is obtained by setting m_0 to ∞ in $H_{\rm nr}^{\rm int}$. Such a Hamiltonian is used in standard atomic nonrelativistic calculations based on the Born-Oppenheimer approximation. We used both FNM and INM Hamiltonians in the present calculations to obtain the energies of ^{10}B and ^{11}B, as well as of $^{\infty}$B. If the FNM Hamiltonian is used, the energy and the corresponding wave function depend on the mass of the nucleus. Thus the results are specific to a particular isotope.

Hamiltonian (1) can also be written in a compact matrix form [17] as

$$H_{\rm nr}^{\rm int} = -\nabla_{\mathbf{r}}' \mathbf{M} \nabla_{\mathbf{r}} + \sum_{i=1}^{n} \frac{q_0 q_i}{\mathbf{r}_i} + \sum_{i=1}^{n} \sum_{j<i}^{n} \frac{q_i q_j}{\mathbf{r}_{ij}}, \tag{2}$$

where

$$\nabla_{\mathbf{r}} = \begin{pmatrix} \nabla_{\mathbf{r}_1} \\ \nabla_{\mathbf{r}_2} \\ \vdots \\ \nabla_{\mathbf{r}_n} \end{pmatrix}$$

is a $3n$-component gradient vector and $\mathbf{M} = M \otimes I_3$ is the Kronecker product of an $n \times n$ matrix M and 3×3 identity matrix I_3. The diagonal elements of matrix M are $1/(2\mu_1), 1/(2\mu_2), \ldots, 1/(2\mu_n)$ and all off-diagonal elements are equal to $1/(2m_0)$.

B. Basis functions

All-electron explicitly correlated Gaussian basis functions are used to expand the spatial part of the wave function for each of the considered ^2S states of boron. The ECGs have the following form [this form is equivalent to Eq. (4)]:

$$\phi_k = \exp\left[-\mathbf{r}'(A_k \otimes I_3)\mathbf{r}\right], \tag{3}$$

where $\mathbf{r}$ is a $3n$ vector of the internal electron coordinates,

$$\mathbf{r} = \begin{pmatrix} \mathbf{r}_1 \\ \mathbf{r}_2 \\ \vdots \\ \mathbf{r}_n \end{pmatrix},$$

A_k is an $n \times n$ real symmetric matrix, $\otimes$ is the Kronecker product, and I_3 is a 3×3 identity matrix. The prime symbol denotes the matrix or vector transpose. The square integrability of functions (3) is required, as they are used expand wave functions of bound stationary states. It means A_k has to be positive definite. To achieve this, A_k is represented in a Cholesky-factored form as $A_k = L_k L_k'$, where L_k is a lower triangular matrix with all matrix elements being real numbers that can be varied in the range from $-\infty$ to ∞. Thus, there is no need to impose any constraints on the lower-triangle L_k matrix elements to make A_k positive definite. The matrix elements of L_k's are the variational parameters that are optimized in the variational energy minimizations performed in this work.

As stated in the Introduction, effective atomic explicitly correlated basis functions should be capable of describing the decrease of the probability of any two electrons being found close to each other. To analyze whether ECGs have this property, let us consider, for example, the ground state of the helium atom. An ECG for this case can be written as

$$\psi(1,2) = \exp\left(-\alpha_1 r_1^2 - \alpha_2 r_2^2 - \beta r_{12}^2\right), \tag{4}$$

where α_1, α_2, and β are parameters, r_1 and r_2 are the distances of electron 1 and electron 2 from the nucleus, respectively, and r_{12} is the distance between the electrons. One notices that the Gaussian has a maximum at $r_{12} = 0$, but the wave function should have a minimum at this distance. One way of achieving that is by multiplying Eq. (4) by an r_{12}-dependent function that makes $\psi(1,2)$ go to zero when $r_{12} \to 0$. A possible multiplier can be r_{12}^2. We considered such a multiplier in one of our previous works [31]. One way of introducing such a multiplier to function (4) is by differentiating $\psi(1,2)$ with respect to $-\beta$. As it was indeed shown in Ref. [31] by including functions (4) in the basis set used in the calculation of the ground state of the He atom along with functions $r_{12}^2\psi(1,2)$ one can accelerate the energy convergence in terms of the number of basis functions. If ECGs with the r_{12}^2 preexponential multiplier are not included in the basis set, as it is done in the present calculations, there is a tendency of the variational optimization to make some basis functions linearly dependent. This happens because an approximate way to generate basis functions with the r_{12}^2 preexponential multipliers is by the following 'numerical" differentiation, which the variational optimization exploits to lower the energy of the system:

$$r_{12}^2\psi(1,2) \approx \lim_{\delta\to 0}\left(\exp\left(-\alpha_1 r_1^2 - \alpha_2 r_2^2 - (\beta+\delta) r_{12}^2\right) - \exp\left(-\alpha_1 r_1^2 - \alpha_2 r_2^2 - \beta r_{12}^2\right)\right)/(-\delta). \tag{5}$$

Note that, at $\delta \to 0$, the two functions in Eq. (5) become linearly dependent.

In this work we use the spin-free formalism to implement the appropriate permutational symmetry of the wave function and to properly evaluate all necessary matrix elements. In this formalism, the desired symmetry properties of the wave function are implemented by applying an appropriate symmetry projector to each ECG basis function. The projector is constructed using the standard procedure employing Young operators (see Ref. [32]). In the calculation of ^2S states of the boron atom, the projector can be chosen as $P = (1 - P_{13})(1 - P_{15} - P_{35})(1 - P_{24})(1 + P_{12})(1 + P_{34})$, where P_{ij} permutes the spatial coordinates of electrons i and j. In the calculation of an expectation value of an operator, which is fully symmetric with respect to permuting electron labels (all operators used in the present work are like that), the P operator can be moved from the bra side of the integral to the ket side. Thus, the symmetry projection appears only on the ket side in the form of $P^\dagger P$. As this projection contains $5! = 120$ terms, each matrix element calculated in this work consists of 120 different elemental spatial integrals.

In the present work, we also estimate the nonrelativistic and total energies at a complete basis size. An analysis of the procedure used to grow and optimize the basis sets in the present calculations shows that the differences between the consecutive nonrelativistic energies obtained with the

TABLE I. The extrapolated ^{11}B nonrelativistic energy to infinite basis set size of the $2s^2 3s$ state. The numbers in parentheses represent the uncertainty in the extrapolated energy.

n	Basis size	E_{nr}	$\Delta E_{n,n-1}$	q
1	10000	−24.470143631		
2	12000	−24.470143683	-5.13×10^{-8}	
3	14000	−24.470143716	-3.39×10^{-8}	0.66
4	16000	−24.470143748	-2.39×10^{-8}	0.70
	∞	−24.470143779(16)		

incrementally increased number of the basis functions behaves approximately as a geometric series. Based on this observation, the following formula is used to estimate the energy value at an infinite number of the basis functions:

$$E_\infty = E_4 + \Delta E_{4,3}\frac{q_4}{1-q_4}, \tag{6}$$

where

$$q_n = \frac{\Delta E_{n,n-1}}{\Delta E_{n-1,n-2}},$$
$$\Delta E_{n,n-1} = E_n - E_{n-1}.$$

Equation (6) shows how the extrapolated energy value, E_∞, is obtained from energies E_4, E_3, and E_2, where E_4 is the energy obtained with the largest basis set generated for a given state, E_3 is the energy obtained with the next largest basis set (for example, the basis set with the number of the basis functions by two thousands smaller than the largest basis set), and E_2 is the energy obtained with next largest basis set (i.e., the basis set by four thousands smaller than the largest). Table I shows an example of the application of the extrapolation procedure to estimate E_∞ for the lowest ^2S state ($2s^2 3s$) of the ^{11}B isotope.

C. The leading relativistic and QED energy corrections

Calculations performed at the nonrelativistic level of the theory, even if they are very accurate, are insufficient to determine the total energies and the interstate transition energies with an accuracy comparable with the present-day spectroscopic results. To achieve spectroscopic accuracy, at least the leading relativistic and QED energy corrections need to be included in the calculations. An approach to account for these corrections that is practical and most frequently used in calculating bound states of light atoms is based on expanding the total energy of the atom in terms of powers of the fine-structure constant, α [33,34]:

$$E_{\rm tot} = E_{\rm nr} + \alpha^2 E^{(2)}_{\rm rel} + \alpha^3 E^{(3)}_{\rm QED} + \alpha^4 E^{(4)}_{\rm HQED} + \cdots, \tag{7}$$

where $E_{\rm nr}$ is the nonrelativistic energy of the considered state, $\alpha^2 E^{(2)}_{\rm rel}$ represents the leading relativistic corrections, $\alpha^3 E^{(3)}_{\rm QED}$ represents the leading QED corrections, and $\alpha^4 E^{(4)}_{\rm HQED}$ represents higher-order QED corrections. The relativistic and QED corrections are obtained as expectation values of some effective operators representing them. In particular, $E^{(2)}_{\rm rel}$ is calculated as the expectation value of the Dirac-Breit Hamiltonian in the Pauli approximation, $H_{\rm rel}$ [35,36]. In the present study of the ^2S states of boron, $H_{\rm rel}$ contains the following terms:

$$H_{\rm rel} = H_{\rm MV} + H_{\rm D} + H_{\rm OO} + H_{\rm SS}, \tag{8}$$

where $H_{\rm MV}$, $H_{\rm D}$, $H_{\rm OO}$, and $H_{\rm SS}$ are operators representing the mass-velocity, Darwin, orbit-orbit, and spin-spin effects, respectively. In the internal Cartesian coordinate system, the operators have the form given in our previous works [37,38]. Due to the use of the finite-nuclear-mass approach is the present work, nuclear-mass dependency appears in the above operators. The nonrelativistic wave functions used in calculating the expectation values are also nuclear-mass dependent. Thus, the values of the relativistic corrections are specific to a particular isotope (^{10}B or ^{11}B); i.e., as mentioned, the so-called recoil effects are directly included in these corrections.

The leading QED correction, $E^{(3)}_{\rm QED}$ in Eq. (7), represents the two-photon exchange, vacuum polarization, and electron self-energy effects. The corresponding operator is expressed as a combination of two sums:

$$H_{\rm QED} = \sum_{\substack{i,j=1\\ j>i}}^{n}\left[\left(\frac{164}{15}+\frac{14}{3}\ln\alpha\right)\delta(\mathbf{r}_{ij}) - \frac{7}{6\pi}\mathcal{P}\left(\frac{1}{r_{ij}^3}\right)\right] + \sum_{i=1}^{n}\left(\frac{19}{30} - 2\ln\alpha - \ln k_0\right)\frac{4q_0}{3}\delta(\mathbf{r}_i). \tag{9}$$

The first sum is the so-called Araki-Sucher term [39–43], where the principal value $\mathcal{P}\,(1/r_{ij}^3)$ is defined as

$$\left\langle\mathcal{P}\left(\frac{1}{r_{ij}^3}\right)\right\rangle = \lim_{a\to0}\left\langle\frac{1}{r_{ij}^3}\Theta(r_{ij}-a) + 4\pi(\gamma+\ln a)\delta(\mathbf{r}_{ij})\right\rangle. \tag{10}$$

In the last expression $\Theta(\cdots)$ is the Heaviside step function and $\gamma = 0.577215\ldots$ is the Euler-Mascheroni constant.

The dominant part of the self-energy term includes the so-called Bethe logarithm, $\ln k_0$. This logarithm is notoriously difficult to calculate for a multielectron atomic system. The main contribution to $\ln k_0$ comes from the inner-shell electrons. The $\ln k_0$ values used in the present calculations are taken from our previous work on the lowest four ^2S states of boron [44]. For the fifth and higher states, the value of $\ln k_0$ for the fourth excited state is used. This is because $\ln k_0$ changes little for higher excited states. The second term in Eq. (9) is calculated directly from the formula.

In the calculation of the $E^{(4)}_{\rm HQED}$ term in expansion (7), the following approximate operator derived by Pachucki *et al.* [45,46] is used:

$$H_{\rm HQED} = \pi q_0^2\left(\frac{427}{96} - 2\ln 2\right)\sum_{i=1}^{3}\delta(\mathbf{r}_i), \tag{11}$$

where $H_{\rm HQED}$ represents the dominating electron-nucleus one-loop radiative correction. The two-loop radiative, electron-electron radiative, and the higher-order relativistic corrections are neglected. The approximate operator of Pachucki *et al.* only provides a rough estimate of $E^{(4)}_{\rm HQED} = \langle\psi|H_{\rm HQED}|\psi\rangle$.

It seems that the importance of the neglected terms significantly increases with the increasing size of the system. For

TABLE II. Nonrelativistic and total energies computed with the largest basis sets of 16 000 ECGs along with their extrapolated values. All energies are in atomic units.

Isotope	Basis	State	E_{nr}	E_{tot}	State	E_{nr}	E_{tot}
^{10}B	16000	$2s^23s$	−24.470019349	−24.475613348	$2s^27s$	−24.3602021	−24.3657287
	∞		−24.470019371(12)	−24.475613371(12)		−24.3602055(12)	−24.3657321(12)
^{11}B	16000		−24.470143748	−24.475737735		−24.3603253	−24.3658518
	∞		−24.470143771(12)	−24.475737758(12)		−24.3603286(12)	−24.3658551(12)
$^{\infty}$B	16000		−24.471393641	−24.476987496		−24.3615625	−24.3670880
	∞		−24.471393664(12)	−24.476987519(12)		−24.3615658(12)	−24.3670914(12)
^{10}B	16000	$2s^24s$	−24.401819489	−24.407402733	$2s^28s$	−24.3572446	−24.3628173
	∞		−24.401819720(35)	−24.407402962(35)		−24.3572555(20)	−24.3628284(20)
^{11}B	16000		−24.401943485	−24.407526717		−24.3573682	−24.3629409
	∞		−24.401943716(35)	−24.407526946(35)		−24.3573792(20)	−24.3629520(20)
$^{\infty}$B	16000		−24.403189329	−24.408772432		−24.3586104	−24.3641829
	∞		−24.403189560(35)	−24.408772661(35)		−24.3586214(20)	−24.3641940(20)
^{10}B	16000	$2s^25s$	−24.37842403	−24.38400019	$2s^29s$	−24.3550304	−24.3606108
	∞		−24.37842476(15)	−24.38400088(15)		−24.3550646(53)	−24.3606452(53)
^{11}B	16000		−24.37854784	−24.38412400		−24.3551541	−24.3607345
	∞		−24.37854858(15)	−24.38412469(15)		−24.3551883(53)	−24.3607689(53)
$^{\infty}$B	16000		−24.37979190	−24.38536794		−24.3563971	−24.3619773
	∞		−24.37979263(15)	−24.38536864(15)		−24.3564313(53)	−24.3620117(53)
^{10}B	16000	$2s^26s$	−24.36780237	−24.37335494	$2s^210s$	−24.353414	−24.358997
	∞		−24.36780393(35)	−24.37335642(35)		−24.353489(11)	−24.359072(11)
^{11}B	16000		−24.36792589	−24.37347848		−24.353538	−24.359121
	∞		−24.36792746(35)	−24.37347996(35)		−24.353613(11)	−24.359196(11)
$^{\infty}$B	16000		−24.36916705	−24.37471972		−24.354781	−24.360364
	∞		−24.36916862(35)	−24.37472121(35)		−24.354856(11)	−24.360439(11)
^{10}B	16000	$2s2p^2$	−24.36297694	−24.36843959	$2s^211s$	−24.352204	−24.357787
	∞		−24.36297943(70)	−24.36844211(70)		−24.352266(23)	−24.357849(23)
^{11}B	16000		−24.36309947	−24.36856212		−24.352327	−24.357911
	∞		−24.36310196(70)	−24.36856464(70)		−24.352390(23)	−24.357973(23)
$^{\infty}$B	16000		−24.36433059	−24.36979319		−24.353571	−24.359154
	∞		−24.36433309(70)	−24.36979580(70)		−24.353633(23)	−24.359216(23)

instance, 10% and 20% errors were estimated in the calculated values for the Li [47] and Be [48] atoms, respectively. Unfortunately, there is no reliable way to estimate the error of the computed HQED corrections for such multielectron atoms as beryllium and boron. However, a prudent analysis allows to determine that the overall error is likely be less than 50%.

The formalism for calculating the expectation values of the H_{QED} and H_{HQED} Hamiltonians was developed under the assumption of a clamped nucleus [45,46]. Thus, in the present work, the infinite-nuclear-mass wave functions are used to calculate these terms. It means that the relativistic corrections calculated in this work include the recoil effects; these effects are absent in the QED corrections.

Some of the relativistic and QED operators include singular terms. $\nabla^4_{\mathbf{r}_i}$, $\delta(\mathbf{r}_i)$, and $\delta(\mathbf{r}_{ij})$ [note that $\delta(\mathbf{r}_i) \equiv \delta(x_i)\delta(y_i)\delta(z_i)$] are such terms. The expectation values of singular operators usually converge much slower with the number of the basis functions used to expand the wave function than the expectation values of nonsingular operators. The slow convergence is mainly due to the local character of the singular operators, i.e., their expectation values depend on the accuracy of small fragments of the wave function rather than on the overall accuracy of the wave function. For approximate wave functions, local errors may be considerably more significant than the global error. Thus, in the calculations of the expectation values of local and singular operators with such wave functions, the error can be larger than the error of the expectation values calculated for such global operators as, for example, the Hamiltonian. This behavior, in general, may occur regardless of the basis set employed in the calculation. To reduce the accuracy loss in the calculations of the expectation values of local and singular operators, it was proposed to replace these operators by equivalent operators but less singular and less local [49–54]. Drachman proposed the so-called regularization approach, to construct such replacement operators [54] based on the work of Trivedi [53] that made use of an expectation value identity. In the limit of the exact wave function, the original operators and the replacement operators give the same expectation values, while for approximate wave functions the expectation values of the replacement operators are usually much closer to the exact values than expectation values of the original operators. The regularization approach of Drachman is particularly useful and effective in calculating expectation values of the operators representing the leading relativistic and QED corrections with wave functions expanded in terms of ECGs [21,38], as well as other types of explicitly correlated basis functions [55,56]. For ECGs, the application of the regularization method is

TABLE III. Some key expectation values (all in atomic units) for the ten lowest ^2S states of ^{10}B, ^{11}B, and $^{\infty}$B isotopes computed with the largest basis sets of 16 000 ECG functions used in this work. The tilde sign indicates that the regularization technique was used to compute the expectation value. The numbers in parentheses are estimated uncertainties due to the basis truncation.

State	Isotope	$\langle\tilde{H}_{\rm MV}\rangle$	$\langle\tilde{\delta}(\mathbf{r}_i)\rangle$	$\langle\tilde{\delta}(\mathbf{r}_{ij})\rangle$	$\langle H_{\rm OO}\rangle$	$\langle\mathcal{P}(1/r_{ij}^3)\rangle$
$2s^23s$	^{10}B	−700.20717(1)	14.50655656(4)	0.358158660(6)	−1.5600823(2)	
	^{11}B	−700.22129(1)	14.50677540(4)	0.358163425(6)	−1.5544572(2)	
	$^{\infty}$B	−700.36320(1)	14.50897429(4)	0.358211305(6)	−1.4979332(2)	−2.94366(3)
$2s^24s$	^{10}B	−699.5466(1)	14.4955059(3)	0.357662320(14)	−1.5575239(16)	
	^{11}B	−699.5607(1)	14.4957250(3)	0.357667096(14)	−1.5519057(16)	
	$^{\infty}$B	−699.7028(1)	14.4979274(3)	0.357715092(14)	−1.4954514(16)	−2.9498(3)
$2s^25s$	^{10}B	−699.0559(5)	14.4865338(27)	0.357319393(63)	−1.5427622(90)	
	^{11}B	−699.0702(5)	14.4867559(27)	0.357324270(63)	−1.5371553(90)	
	$^{\infty}$B	−699.2137(5)	14.4889867(27)	0.357373266(63)	−1.4808133(90)	−2.9565(16)
$2s^26s$	^{10}B	−697.3229(24)	14.45369(2)	0.3561490(6)	−1.47043(7)	
	^{11}B	−697.3384(24)	14.45393(2)	0.3561548(6)	−1.46489(7)	
	$^{\infty}$B	−697.4946(24)	14.45641(2)	0.3562123(6)	−1.40928(7)	−2.9313(33)
$2s2p^2$	^{10}B	−690.658(9)	14.32680(17)	0.3516566(61)	−1.18373(36)	
	^{11}B	−690.673(9)	14.32703(17)	0.3516617(61)	−1.17823(36)	
	$^{\infty}$B	−690.819(9)	14.32932(17)	0.3517127(61)	−1.12291(36)	−2.8384(14)
$2s^27s$	^{10}B	−695.398(8)	14.41711(17)	0.3548454(64)	−1.38832(28)	
	^{11}B	−695.407(8)	14.41722(17)	0.3548463(64)	−1.38249(28)	
	$^{\infty}$B	−695.491(8)	14.41832(17)	0.3548554(64)	−1.32397(28)	−2.9145(44)
$2s^28s$	^{10}B	−698.831(7)	14.48252(13)	0.3571581(81)	−1.53700(9)	
	^{11}B	−698.844(7)	14.48272(13)	0.3571621(81)	−1.53133(9)	
	$^{\infty}$B	−698.975(7)	14.48471(13)	0.3572027(81)	−1.47445(9)	−2.9698(82)
$2s^29s$	^{10}B	−699.389(15)	14.49308(38)	0.3575290(174)	−1.56135(6)	
	^{11}B	−699.403(15)	14.49329(38)	0.3575335(174)	−1.55571(6)	
	$^{\infty}$B	−699.541(15)	14.49543(38)	0.3575790(174)	−1.49906(6)	−3.0022(172)
$2s^210s$	^{10}B	−699.538(38)	14.49581(76)	0.3576238(319)	−1.56808(10)	
	^{11}B	−699.552(38)	14.49602(76)	0.3576284(319)	−1.56244(10)	
	$^{\infty}$B	−699.692(38)	14.49819(76)	0.3576749(319)	−1.50582(10)	−3.0416(204)
$2s^211s$	^{10}B	−699.590(68)	14.49684(98)	0.3576609(269)	−1.57089(53)	
	^{11}B	−699.604(68)	14.49706(98)	0.3576655(269)	−1.56526(53)	
	$^{\infty}$B	−699.745(68)	14.49923(98)	0.3577126(269)	−1.50865(53)	−3.0524(82)

particularly important, as these functions to not satisfy the Kato's cusp conditions. The regularization method is used in the present calculations.

III. RESULTS

The present calculations have been performed on several multiprocessor computers and have lasted multiple months. Most of the computer time is used to grow the basis set and to optimize the nonlinear parameters of the basis functions. The basis set is independently and separately grown and optimized for each of the ten considered ^2S states of boron to the size of 16 000 functions. The approach used in the optimization was described in our previous works (see, for example, Ref. [44]). The calculations are done using the extended computer precision of 10 bytes per real number (an extension from the double precision of 8 bytes per number). The increase of the precision accelerates the convergence of the calculation. This is likely due to more precise evaluation of the energy gradient. The optimization of the basis sets is carried out for the ^{11}B isotope of boron. This basis set is then used to perform calculations for the ^{10}B isotope and for $^{\infty}$B, i.e., for the boron atom with an infinite nuclear mass. In our previous paper [44] we presented calculations for the lowest four ^2S states of boron. The largest basis-set size used there was 15 000. Increasing the basis-set size to 16 000, employing the extended precision in the calculations, and performing several additional optimization cycles for the 16 000-ECG basis set for each state resulted in a noticeable decrease of the variational nonrelativistic energies of the four states (see the results presented in Table II). For the lowest $2s^23s$ state, the ^{11}B energy decreased from −24.470143729 to −24.470143748 a.u., for the $2s^24s$ state the energy decreased from −24.401943437 to −24.401943485 a.u., for the $2s^25s$ state the energy decreased from −24.378547683 to −24.37854784 a.u., and for the $2s^26s$ state the energy decreased from −24.367925311 to −24.36792589 a.u. Also, in the present calculations, the range of the calculated ^2S states is extended to include the next six higher states, i.e., the $2s2p^2$ states and the $2s^2ns$ states with $n = 7, \ldots, 11$.

The nonrelativistic energies, E_{nr}, for all ten states of ^{10}B, ^{11}B, and $^{\infty}$B are shown in Table II. As one can see, the

TABLE IV. Transition energies, ΔE (in cm^{-1}), for adjacent ^2S states of the ^{10}B and ^{11}B isotopes of boron computed using infinite-nuclear-mass (i) nonrelativistic energies (nr) and then gradually increasing the accuracy of the calculations by including the finite-nuclear-mass (f), relativistic (rel), and QED effects. As the QED and HQED operators used in the present work are only valid for the infinite-nuclear-mass (INM) model, the corresponding energy corrections are computed using the wave functions obtained in the INM calculations. The estimated uncertainties shown for the extrapolated transition energies are due to the basis truncation.

Isotope	Contributions included in ΔE	Basis size	$2s^23s \leftarrow 2s^24s$	$2s^24s \leftarrow 2s^25s$	$2s^25s \leftarrow 2s^26s$	$2s^26s \leftarrow 2s2p^2$	$2s2p^2 \leftarrow 2s^27s$
^{10}B	nr(i)	16000	14969.116	5135.143	2331.883	1061.481	607.528
	nr(f)	16000	14968.139	5134.711	2331.185	1059.058	609.005
	nr(f) + rel(f)	16000	14970.635	5136.375	2336.779	1080.418	593.830
	nr(f) + rel(f) + QED(i)	16000	14970.508	5136.272	2336.387	1078.889	594.904
	nr(f) + rel(f) + QED(i) + HQED(i)	16000	14970.500	5136.265	2336.362	1078.794	594.971
	nr(f) + rel(f) + QED(i) + HQED(i)	∞	14970.454(10)	5136.163(42)	2336.19(11)	1078.57(23)	594.8(4)
	Experiment [57]		14970.47(9)	5136.16(10)	2335.74(15)	1078.47(21)	595.38(21)
			$2s^27s \leftarrow 2s^28s$	$2s^28s \leftarrow 2s^29s$	$2s^29s \leftarrow 2s^210s$	$2s^210s \leftarrow 2s^211s$	
	nr(i)	16000	647.902	485.772	354.599	265.753	
	nr(f)	16000	649.108	485.961	354.645	265.766	
	nr(f) + rel(f)	16000	638.122	484.141	354.107	265.613	
	nr(f) + rel(f) + QED(i)	16000	638.923	484.278	354.152	265.628	
	nr(f) + rel(f) + QED(i) + HQED(i)	16000	638.973	484.286	354.154	265.629	
	nr(f) + rel(f) + QED(i) + HQED(i)	∞	637.3(7)	479.2(16)	345(4)	268(8)	
Isotope	Contributions included in ΔE	Basis size	$2s^23s \leftarrow 2s^24s$	$2s^24s \leftarrow 2s^25s$	$2s^25s \leftarrow 2s^26s$	$2s^26s \leftarrow 2s2p^2$	$2s2p^2 \leftarrow 2s^27s$
^{11}B	nr(i)	16000	14969.116	5135.143	2331.883	1061.481	607.528
	nr(f)	16000	14968.228	5134.750	2331.248	1059.277	608.871
	nr(f) + rel(f)	16000	14970.724	5136.413	2336.838	1080.640	593.715
	nr(f) + rel(f) + QED(i)	16000	14970.596	5136.310	2336.446	1079.111	594.789
	nr(f) + rel(f) + QED(i) + HQED(i)	16000	14970.588	5136.303	2336.422	1079.016	594.856
	nr(f) + rel(f) + QED(i) + HQED(i)	∞	14970.543(10)	5136.202(42)	2336.25(11)	1078.78(23)	594.7(4)
	Experiment [57]		14970.561(24)	5136.186(29)	2335.76(14)	1078.47(20)	595.38(21)
			$2s^27s \leftarrow 2s^28s$	$2s^28s \leftarrow 2s^29s$	$2s^29s \leftarrow 2s^210s$	$2s^210s \leftarrow 2s^211s$	
	nr(i)	16000	647.902	485.772	354.599	265.753	
	nr(f)	16000	648.999	485.944	354.640	265.765	
	nr(f) + rel(f)	16000	637.999	484.121	354.102	265.611	
	nr(f) + rel(f) + QED(i)	16000	638.800	484.258	354.147	265.627	
	nr(f) + rel(f) + QED(i) + HQED(i)	16000	638.849	484.266	354.149	265.628	
	nr(f) + rel(f) + QED(i) + HQED(i)	∞	637.2(7)	479.1(16)	345(4)	268(8)	
Isotope	Contributions included in ΔE	Basis size	$2s^23s \leftarrow 2s^24s$	$2s^24s \leftarrow 2s^25s$	$2s^25s \leftarrow 2s^26s$	$2s^26s \leftarrow 2s2p^2$	$2s2p^2 \leftarrow 2s^27s$
Natural	nr(f) + rel(f) + QED(i) + HQED(i)	∞	14970.525(15)	5136.194(59)	2336.24(61)	1078.74(33)	594.69(58)
mixture	Experiment [57]		14970.5431(33)	5136.180(10)	2335.75(14)	1078.47(20)	595.38(21)
			$2s^27s \leftarrow 2s^28s$	$2s^28s \leftarrow 2s^29s$	$2s^29s \leftarrow 2s^210s$	$2s^210s \leftarrow 2s^211s$	
	nr(f) + rel(f) + QED(i) + HQED(i)	∞	637.19(98)	479.1(23)	345(5)	268(10)	
	Experiment [57]		636.07(21)	478.10(21)	339.19(21)		

number of the significant figures shown in the energy values for each state decreases with the level of excitation. This reflects the slowing of the energy convergence rate with the number of basis functions as more radial nodes appear in the wave function. For each state of each isotope, the energy value extrapolated to an infinite number of the basis functions is also shown in the table along with the corresponding estimated uncertainty. In the table, we also show the total energies of the states calculated as the sum of the nonrelativistic energy and the relativistic and QED corrections. The values of the quantities that are used to calculate these corrections are shown in Table III. These quantities, which are calculated with the largest basis set of 16 000 ECG, include the expectation value of the mass-velocity operator, the expectation values of the one- and two-electron Dirac delta functions, $\langle\tilde{\delta}(\mathbf{r}_i)\rangle$ and $\langle\tilde{\delta}(\mathbf{r}_{ij})\rangle$, the expectation value of the orbit-orbit magnetic interaction operator, $\langle H_{OO}\rangle$, and the expectation value of the distribution used to calculate the first term of the leading QED correction, $\langle\mathcal{P}(1/r_{ij}^3)\rangle$. In the table, the expectation values are shown for all ten ^2S states considered for ^{10}B, ^{11}B, and $^{\infty}$B. For each expectation value, an estimated uncertainty is given in parentheses. Here again, due to the decreasing accuracy with increasing level of electronic excitation, the number of the significant figures in the expectation value decreases from eight for the $2s^23s$ state to six for the $2s^211s$ state.

The next set of results concerns transition energies corresponding to all pairs of the adjacent states. The energies are

TABLE V. Transition energies, ΔE (in cm^{-1}), for the $2s^23s$ and higher ^2S states of the ^{10}B and ^{11}B isotopes of boron computed using infinite-nuclear-mass (i) nonrelativistic energies (nr), and then gradually increasing the accuracy of the calculations by including the finite nuclear mass (f), relativistic (rel), and QED effects. As the QED and HQED operators used in the present work are only valid for the infinite-nuclear-mass (INM) model, the corresponding energy corrections are computed using the wave functions obtained in the INM calculations. The estimated uncertainties shown for the extrapolated transition energies are due to the basis truncation.

Isotope	Contributions included in ΔE	Basis size	$2s^23s \leftarrow 2s^24s$	$2s^23s \leftarrow 2s^25s$	$2s^23s \leftarrow 2s^26s$	$2s^23s \leftarrow 2s2p^2$	$2s^23s \leftarrow 2s^27s$
^{10}B	nr(i)	16000	14969.116	20104.259	22436.142	23497.624	24105.151
	nr(f)	16000	14968.139	20102.850	22434.035	23493.093	24102.098
	nr(f) + rel(f)	16000	14970.635	20107.010	22443.789	23524.207	24118.037
	nr(f) + rel(f) + QED(i)	16000	14970.508	20106.779	22443.166	23522.055	24116.959
	nr(f) + rel(f) + QED(i) + HQED(i)	16000	14970.500	20106.764	22443.127	23521.921	24116.891
	nr(f) + rel(f) + QED(i) + HQED(i)	∞	14970.454(10)	20106.618(36)	22442.807(80)	23521.37(15)	24116.15(26)
	Experiment, [57]		14970.47(9)	20106.63(5)	22442.37(14)	23520.84(15)	24116.22(15)
			$2s^23s \leftarrow 2s^28s$	$2s^23s \leftarrow 2s^29s$	$2s^23s \leftarrow 2s^210s$	$2s^23s \leftarrow 2s^211s$	
	nr(i)	16000	24753.053	25238.825	25593.425	25859.177	
	nr(f)	16000	24751.206	25237.168	25591.812	25857.579	
	nr(f) + rel(f)	16000	24756.159	25240.299	25594.406	25860.019	
	nr(f) + rel(f) + QED(i)	16000	24755.882	25240.160	25594.311	25859.940	
	nr(f) + rel(f) + QED(i) + HQED(i)	16000	24755.864	25240.150	25594.303	25859.933	
	nr(f) + rel(f) + QED(i) + HQED(i)	∞	24753.44(44)	25232.6(12)	25577.8(25)	25846.2(50)	
Isotope	Contributions included in ΔE	Basis size	$2s^23s \leftarrow 2s^24s$	$2s^23s \leftarrow 2s^25s$	$2s^23s \leftarrow 2s^26s$	$2s^23s \leftarrow 2s2p^2$	$2s^23s \leftarrow 2s^27s$
^{11}B	nr(i)	16000	14969.116	20104.259	22436.142	23497.624	24105.151
	nr(f)	16000	14968.228	20102.977	22434.226	23493.503	24102.374
	nr(f) + rel(f)	16000	14970.724	20107.137	22443.975	23524.615	24118.330
	nr(f) + rel(f) + QED(i)	16000	14970.596	20106.906	22443.353	23522.463	24117.253
	nr(f) + rel(f) + QED(i) + HQED(i)	16000	14970.588	20106.891	22443.313	23522.329	24117.185
	nr(f) + rel(f) + QED(i) + HQED(i)	∞	14970.543(10)	20106.745(36)	22442.993(80)	23521.78(16)	24116.45(26)
	Experiment, [57]		14970.561(24)	20106.747(17)	22442.50(14)	23520.97(14)	24116.35(15)
			$2s^23s \leftarrow 2s^28s$	$2s^23s \leftarrow 2s^29s$	$2s^23s \leftarrow 2s^210s$	$2s^23s \leftarrow 2s^211s$	
	nr(i)	16000	24753.053	25238.825	25593.425	25859.177	
	nr(f)	16000	24751.373	25237.318	25591.958	25857.723	
	nr(f) + rel(f)	16000	24756.329	25240.450	25594.553	25860.164	
	nr(f) + rel(f) + QED(i)	16000	24756.053	25240.311	25594.458	25860.085	
	nr(f) + rel(f) + QED(i) + HQED(i)	16000	24756.034	25240.301	25594.450	25860.078	
	nr(f) + rel(f) + QED(i) + HQED(i)	∞	24753.61(44)	25232.8(12)	25578.0(25)	25846.4(50)	
Isotope	Contributions included in ΔE	Basis size	$2s^23s \leftarrow 2s^24s$	$2s^24s \leftarrow 2s^25s$	$2s^25s \leftarrow 2s^26s$	$2s^26s \leftarrow 2s2p^2$	$2s2p^2 \leftarrow 2s^27s$
Natural	nr(f) + rel(f) + QED(i) + HQED(i)	∞	14970.525(15)	20106.72(52)	22442.96(11)	23521.70(22)	24116.39(36)
mixture	Experiment [57]		14970.5431(33)	20106.723(10)	22442.48(14)	23520.95(14)	24116.33(15)
			$2s^23s \leftarrow 2s^28s$	$2s^23s \leftarrow 2s^29s$	$2s^23s \leftarrow 2s^210s$	$2s^23s \leftarrow 2s^211s$	
	nr(f) + rel(f) + QED(i) + HQED(i)	∞	24753.58(62)	25232.7(16)	25577.9(35)	25846.3(71)	
	Experiment [57]		24752.40(15)	25230.50(15)	25569.69(15)		

shown in Table IV. Each transition energy is calculated at an increasingly more accurate level of theory as the difference between the total energies of the two states involved in the excitation. At the lowest level, the energies are the nonrelativistic variational energies obtained assuming an infinite nuclear mass [nr(i)]. At the next level, the finite-nuclear-mass nonrelativistic energies are used [nr(f)]. At the following level, the energies that are sums of the FNM nonrelativistic energies and the leading relativistic corrections [nr(f) + rel(f)] are used. At the last two levels, we use the energies from the previous step first augmented with the leading QED corrections [nr(f) + rel(f) + QED(f)] and then with the higher-order QED corrections [nr(f) + rel(f) + QED(f) + HQED(i)]. Finally each transition-energy value is extrapolated to an infinite number of the basis functions. The transition energies obtained at all above-mentioned levels of theory for all pairs of the adjacent states within the set of the ten lowest ^2S states considered in the present calculations are shown in Table IV along with the experimental values taken from Ref. [57].

Let us first examine the results for the lowest $2s^23s \leftarrow 2s^24s$ transition for ^{11}B. As one can see, including the finite-nuclear-mass effects lowers the transition energy by about a wave number, but the addition of the relativistic corrections raises the result by about 2.5 cm^{-1}. The addition of the QED corrections lowers the result by about 0.13 cm^{-1}. The final results for the $2s^23s \leftarrow 2s^24s$ transition energy of 14970.588 cm^{-1} (before extrapolation) and of 14970.543(10) cm^{-1} (after extrapolation) agree with the experimental value of 14970.561(24) cm^{-1} well within the

TABLE VI. Expectation values of powers of the interparticle distances, $\langle r_i^p \rangle$ and $\langle r_{ij}^p \rangle$ ($p = -2, -1, 1, 2$), computed with the largest basis sets of 16 000 ECG functions used in this work. All values are in atomic units.

State	Isotope	$\langle r_i^{-2} \rangle$	$\langle r_{ij}^{-2} \rangle$	$\langle r_i^{-1} \rangle$	$\langle r_{ij}^{-1} \rangle$	$\langle r_i \rangle$	$\langle r_{ij} \rangle$	$\langle r_i^2 \rangle$	$\langle r_{ij}^2 \rangle$
$2s^23s$	^{10}B	18.8049330(1)	1.67158086(3)	2.22598196(2)	0.67095104(2)	2.1038338(4)	3.6606569(8)	10.673722(8)	21.77194(2)
	^{11}B	18.8051227(1)	1.67159538(3)	2.22599313(2)	0.67095408(2)	2.1038230(4)	3.6606384(8)	10.673610(8)	21.77172(2)
	$^{\infty}$B	18.8070285(1)	1.67174126(3)	2.22610533(2)	0.67098461(2)	2.1037148(4)	3.6604532(8)	10.672478(8)	21.76948(2)
$2s^24s$	^{10}B	18.7854587(3)	1.65806550(7)	2.20623543(9)	0.6352247(2)	3.598584(7)	6.611332(14)	44.8388(2)	89.9932(4)
	^{11}B	18.7856486(3)	1.65807979(7)	2.20624642(9)	0.6352274(2)	3.598570(7)	6.611306(14)	44.8384(2)	89.9925(4)
	$^{\infty}$B	18.7875571(3)	1.65822345(7)	2.20635682(9)	0.6352542(2)	3.598424(7)	6.611045(14)	44.8345(2)	89.9848(4)
$2s^25s$	^{10}B	18.7748907(22)	1.65553014(11)	2.19953835(53)	0.6231611(12)	5.58004(9)	10.56238(19)	130.655(5)	261.575(9)
	^{11}B	18.7750832(22)	1.65554396(11)	2.19954888(53)	0.6231627(12)	5.58006(9)	10.56242(19)	130.656(5)	261.576(9)
	$^{\infty}$B	18.7770176(22)	1.65568283(11)	2.19965475(53)	0.6231786(12)	5.58027(9)	10.56287(19)	130.660(5)	261.585(9)
$2s^26s$	^{10}B	18.74406(2)	1.658983(2)	2.200445(4)	0.627553(10)	7.465(1)	14.336(2)	273.34(6)	546.93(11)
	^{11}B	18.74427(2)	1.658994(2)	2.200452(4)	0.627546(10)	7.466(1)	14.337(2)	273.37(6)	546.98(11)
	$^{\infty}$B	18.74643(2)	1.659096(2)	2.200523(4)	0.627475(10)	7.471(1)	14.347(2)	273.62(6)	547.49(11)
$2s2p^2$	^{10}B	18.62762(16)	1.677503(28)	2.217449(24)	0.671027(61)	6.318(4)	12.077(8)	283.17(20)	566.65(40)
	^{11}B	18.62781(16)	1.677515(28)	2.217458(24)	0.671026(61)	6.319(4)	12.078(8)	283.19(20)	566.69(40)
	$^{\infty}$B	18.62981(16)	1.677640(28)	2.217553(24)	0.671012(61)	6.321(4)	12.083(8)	283.38(20)	567.09(40)
$2s^27s$	^{10}B	18.70974(7)	1.664058(16)	2.203869(8)	0.637631(21)	10.066(4)	19.548(7)	601.27(58)	1203(1)
	^{11}B	18.70983(7)	1.664089(16)	2.203896(8)	0.637675(21)	10.063(4)	19.541(7)	601.02(58)	1202(1)
	$^{\infty}$B	18.71073(7)	1.664396(16)	2.204171(8)	0.638111(21)	10.027(4)	19.469(7)	598.52(58)	1197(1)
$2s^28s$	^{10}B	18.76946(6)	1.653958(21)	2.193048(2)	0.611170(3)	15.538(21)	30.471(42)	1264(4)	2529(8)
	^{11}B	18.76963(6)	1.653976(21)	2.193062(2)	0.611180(3)	15.537(21)	30.469(42)	1264(4)	2529(8)
	$^{\infty}$B	18.77135(6)	1.654151(21)	2.193204(2)	0.611287(3)	15.527(21)	30.449(42)	1263(4)	2527(8)
$2s^29s$	^{10}B	18.77903(18)	1.652200(40)	2.190590(5)	0.605465(6)	20.5(1)	40.4(2)	2196(30)	4392(60)
	^{11}B	18.77922(18)	1.652215(40)	2.190602(5)	0.605471(6)	20.5(1)	40.4(2)	2196(30)	4392(60)
	$^{\infty}$B	18.78106(18)	1.652369(40)	2.190722(5)	0.605522(6)	20.5(1)	40.4(2)	2195(30)	4391(60)
$2s^210s$	^{10}B	18.78144(36)	1.651736(87)	2.189553(10)	0.603186(6)	26.2(5)	52(1)	3649(154)	7298(307)
	^{11}B	18.78163(36)	1.651751(87)	2.189565(10)	0.603190(6)	26.2(5)	52(1)	3649(154)	7298(307)
	$^{\infty}$B	18.78350(36)	1.651900(87)	2.189680(10)	0.603229(6)	26.2(5)	52(1)	3648(154)	7297(307)
$2s^211s$	^{10}B	18.78231(50)	1.651529(80)	2.188913(74)	0.6018(1)	33.4(17)	66(3)	5996(663)	11993(1325)
	^{11}B	18.78250(50)	1.651543(80)	2.188924(74)	0.6018(1)	33.4(17)	66(3)	5996(663)	11993(1325)
	$^{\infty}$B	18.78439(50)	1.651690(80)	2.189037(74)	0.6019(1)	33.4(17)	66(3)	5996(663)	11993(1325)

experimental uncertainty. The corresponding $2s^24s \leftarrow 2s^25s$ transition energies also agree very well with the experimental value. The agreement is also very good for the first two transitions of ^{10}B. The agreement for the $2s^25s \leftarrow 2s^26s$, $2s^26s \leftarrow 2s2p^2$, and $2s2p^2 \leftarrow 2s^27s$ transitions is somewhat worse, but still the calculated values are within 0.5 cm^{-1} from the experimental results. Note that the experimental uncertainty progressively increases with the level of the electronic excitation, as does the uncertainty of the calculated values. There are no experimental values to make a comparison for the next four transitions.

The total state energies obtained at the various levels of the theory are also used to calculate the transition energies for the second ($2s^24s$) and higher states with respect to the lowest $2s^23s$ state. The results are shown in Table V. Unlike for the transitions between the adjacent states, the values of the transition energies are now increasing with the level of the excitation. However, as one can see, the agreement with experiment is still very good and the discrepancies do not exceed 0.5 cm^{-1} for either ^{10}B or ^{11}B.

Most of the experimental transition energies of the boron atom have been reported for the natural mixture [^{10}B (20%) and ^{11}B (80%)]. Thus, in the present work, we calculate the weighted averages of the transition energies for the naturally occurring mixture of the isotopes. The averages are shown in the bottom parts of Tables IV and V. The experimental and calculated values are compared in the tables. Except for the last transition, all of the calculated values are in a good agreement with the experimental ones and the differences are less than a wave number.

The nonrelativistic wave functions for the ten considered ^2S states of ^{10}B, ^{11}B, and $^{\infty}$B are used to calculate some expectation values of positive and negative powers (ranging from -2 to $+2$) of the nucleus-electron and electron-electron distances. The results are shown in Table VI. Let us focus on the $\langle r_i \rangle$ and $\langle r_{ij} \rangle$ expectation values, i.e., the average nucleus-electron and electron-electron distance, respectively. As expected, both distances increase with the increasing excitation level and the increase accelerates as one moves to higher states. An interesting effect is revealed by comparing the results obtained for the $\langle r_i \rangle$ and $\langle r_{ij} \rangle$ expectation values of the two boron isotopes. It appears that both $\langle r_i \rangle$ and $\langle r_{ij} \rangle$ slightly shrink when the nuclear mass increases (i.e., in going from ^{10}B to ^{11}B). This effect results from the fact that internal motion of the atom is the coupled motion of the electrons and the nucleus around the center of mass of the atom. As the

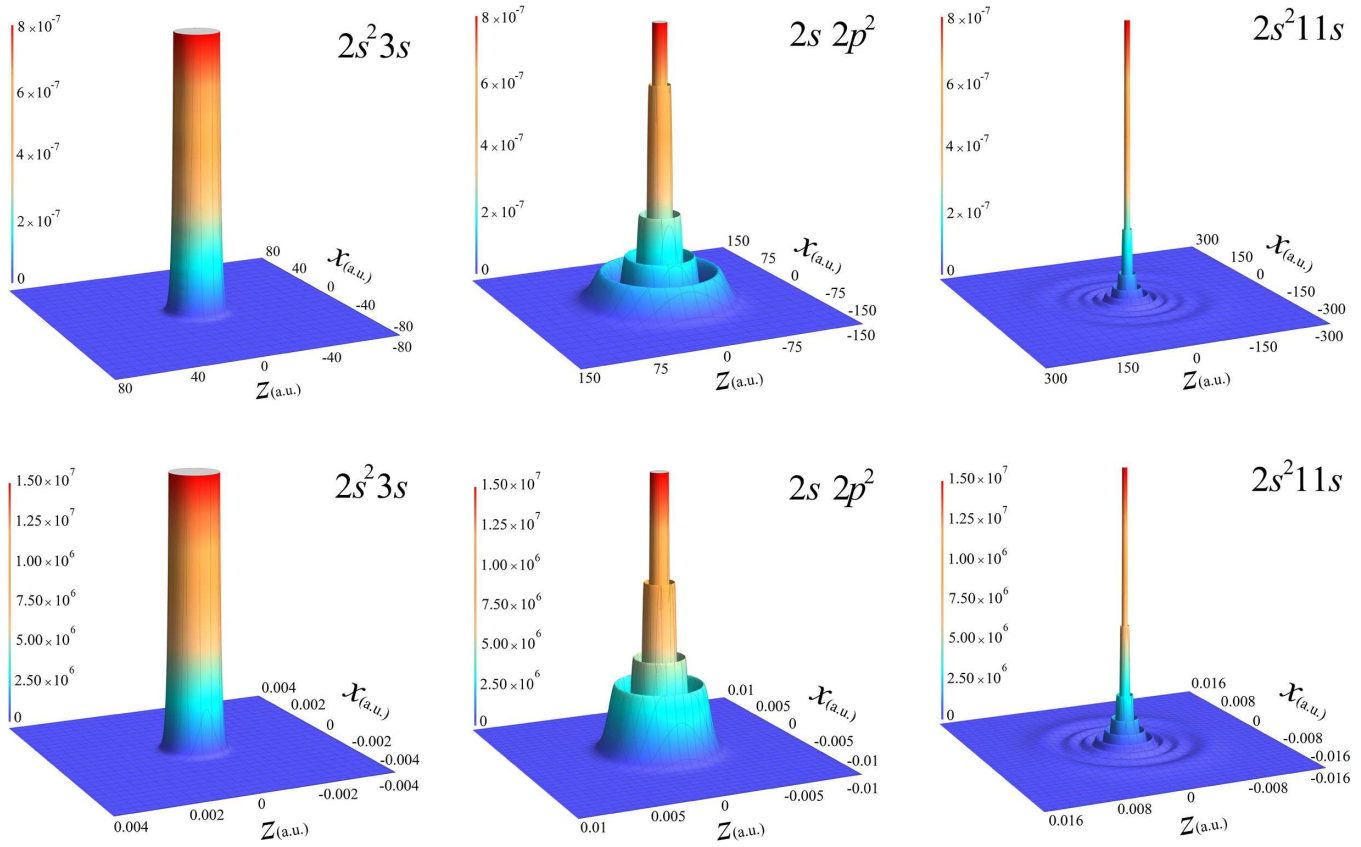

FIG. 1. The density of the electrons (top row) and nucleus (bottom row) in the center-of-mass coordinate frame for the $2s^2 3s$, $2s2p^2$, and $2s^2 11s$ states of the boron atom.

nuclear mass increases, the radius of the motion of the nucleus about the center of mass decreases. When this happens, the average radius of the motion of the electrons about the center of mass also decreases. This results in the atom slightly shrinking and, thus, the nucleus-electron and the electron-electron radii slightly decrease.

An interesting illustration of the coupled nucleus-electron motion in the boron atom is provided by plots of the electronic and nuclear densities. The density of a particle i in the center-of-mass (c.m.) coordinate frame is defined as $\rho_i(\mathbf{r}) = \langle \delta(\mathbf{R}_i - \mathbf{R}_{\text{c.m.}} - \mathbf{r}) \rangle$, where $i = 1, \ldots, N$ and $\mathbf{R}_{\text{c.m.}}$ is the position vector of the center of mass in the laboratory coordinate frame. In this work, the c.m.-frame density plots are generated for both the nucleus and the electrons. When the atom is excited to increasingly higher Rydberg state, the average radius of the electronic density increases, as manifested by the increasing value of the nucleus-electron average distance and by increasing diffuseness of the c.m.-frame electron density. Also, at the same time, the electronic density becomes more oscillatory. The oscillations of the electronic density are mirrored by the oscillations of the c.m.-frame density of the nucleus. The matching number of the maxima in the electronic and nuclear densities for a given state occurs, because only then the center of mass of the atom can remain immobile during the coupled motion of the nucleus and the electrons around the center of mass of the atom. However, due to much larger mass of the nucleus in comparison with the electron mass, the average radius of the nuclear motion around the center of mass is orders of magnitude smaller than the average radius of the motion of the electrons. A pictorial comparison of the two motions using the electronic and nuclear c.m.-frame densities is presented in Fig. 1. The density values are shown for a cross-section plane that includes the center of mass located in the center of the coordinate system used in the plotting. The features to notice in the plots are a visual similarity of the nuclear and electronic densities for each of the three plotted states and the difference in the scales of the two cross-section Cartesian coordinates (X and Z) used in plotting the electronic and nuclear densities.

IV. SUMMARY

Very accurate calculations of the lowest ten ^2S states of two boron stable isotopes, ^{10}B and ^{11}B, are carried out and the interstate transition energies are determined. The results agree well with the high-precision-spectroscopy experimental values. Several months of continuous multiprocessor calculations have been involved in the project. With confidence we can say that the results represent the state of the art of atomic quantum mechanics. The results are the most accurate ever obtained for a spectrum of a five-electron atomic system. The high accuracy of the calculated results is accomplished due to the use of large well-optimized basis sets of all-electron explicitly correlated Gaussian functions. The key feature of the optimization of the Gaussians is the use of the analytical gradient of the energy determined with respect

to the Gaussian nonlinear parameters in the variational energy minimization for the considered state. Augmentation of the nonrelativistic state energies with the leading relativistic and QED corrections calculated using the perturbation-theory approach and not assuming the Born-Oppenheimer approximation in the calculations (i.e., explicitly including the finite-nuclear-mass effects in the nonrelativistic Hamiltonian) are key in achieving the high accuracy of the results.

ACKNOWLEDGMENTS

This work has been supported by Nazarbayev University (faculty development Grant No. 021220FD3651), and the National Science Foundation (Grant No. 1856702).

[1] G. W. F. Drake, M. M. Cassar, and R. A. Nistor, Ground-state energies for helium, H^- and Ps^-, Phys. Rev. A **65**, 054501 (2002).

[2] C. Schwartz, Experiment and theory in computations of the He atom ground state, Int. J. Mod. Phys. E **15**, 877 (2006).

[3] C. Schwartz, Further computations of the He atom ground state, arXiv:math-ph/0605018.

[4] H. Nakashima and H. Nakatsuji, Solving the electron-nuclear Schrödinger equation of helium atom and its isoelectronic ions with the free iterative-complement-interaction method, J. Chem. Phys. **128**, 154107 (2008).

[5] V. A. Yerokhin and K. Pachucki, Theoretical energies of low-lying states of light helium-like ions, Phys. Rev. A **81**, 022507 (2010).

[6] D. T. Aznabaev, A. K. Bekbaev, and V. I. Korobov, Nonrelativistic energy levels of helium atoms, Phys. Rev. A **98**, 012510 (2018).

[7] J. S. Sims and S. A. Hagstrom, Hylleraas-configuration-interaction study of the $2\,^2S$ ground state of neutral lithium and the first five excited ^2S states, Phys. Rev. A **80**, 052507 (2009).

[8] K. Pachucki and A. M. Moro, Nuclear polarizability of helium isotopes in atomic transitions, Phys. Rev. A **75**, 032521 (2007).

[9] M. Puchalski, K. Pachucki, and J. Komasa, Isotope shift in a beryllium atom, Phys. Rev. A **89**, 012506 (2014).

[10] L. M. Wang, Z.-C. Yan, H. X. Qiao, and G. W. F. Drake, Variational energies and the Fermi contact term for the low-lying states of lithium: Basis-set completeness, Phys. Rev. A **85**, 052513 (2012).

[11] M. Puchalski, D. Kędziera, and K. Pachucki, Ground state of Li and Be^+ using explicitly correlated functions, Phys. Rev. A **80**, 032521 (2009).

[12] K. Pachucki and J. Komasa, Excitation energy of ^{9}Be, Phys. Rev. A **73**, 052502 (2006).

[13] H. K. G. Büsse and A. Lüchow, Nonrelativistic energies for the Be atom: Double-linked Hylleraas-CI calculation, Int. J. Quantum Chem. **66**, 241 (1998).

[14] F. W. King, D. Quicker, and J. Langer, Compact wave functions for the beryllium isoelectronic series, Li^- to Ne^{6+}: A standard Hylleraas approach, J. Chem. Phys. **134**, 124114 (2011).

[15] J. Mitroy, S. Bubin, W. Horiuchi, Y. Suzuki, L. Adamowicz, W. Cencek, K. Szalewicz, J. Komasa, D. Blume, and K. Varga, Theory and application of explicitly correlated Gaussians, Rev. Mod. Phys. **85**, 693 (2013).

[16] S. Nasiri, S. Bubin, and L. Adamowicz, in *Chemical Physics and Quantum Chemistry*, Advances in Quantum Chemistry Vol. 81, edited by K. Ruud and E. J. Brändas (Academic Press, New York, 2020), pp. 143–166.

[17] S. Bubin, M. Pavanello, W.-C. Tung, K. L. Sharkey, and L. Adamowicz, Born-Oppenheimer and non-Born-Oppenheimer atomic and molecular calculations with explicitly correlated Gaussians, Chem. Rev. **113**, 36 (2013).

[18] J. Komasa, W. Cencek, and J. Rychlewski, Explicitly correlated Gaussian functions in variational calculations: The ground state of the beryllium atom, Phys. Rev. A **52**, 4500 (1995).

[19] M. Stanke, D. Kędziera, S. Bubin, and L. Adamowicz, Ionization potential of ^{9}Be calculated including nuclear motion and relativistic corrections, Phys. Rev. A **75**, 052510 (2007).

[20] S. Bubin and L. Adamowicz, Assessment of the accuracy the experimental energies of the $^1p^o1s^22s6p$ and $1s^22s7p$ states of ^{9}Be based on variational calculations with explicitly correlated Gaussians, J. Chem. Phys. **137**, 104315 (2012).

[21] K. Pachucki, W. Cencek, and J. Komasa, On the acceleration of the convergence of singular operators in Gaussian basis sets, J. Chem. Phys. **122**, 184101 (2005).

[22] S. Bubin, J. Komasa, M. Stanke, and L. Adamowicz, Isotope shifts of the three lowest ^1s states of the B^+ ion calculated with a finite-nuclear-mass approach and with relativistic and quantum electrodynamics corrections, J. Chem. Phys. **132**, 114109 (2010).

[23] S. Bubin and L. Adamowicz, Correlated-gaussian calculations of the ground and low-lying excited states of the boron atom, Phys. Rev. A **83**, 022505 (2011).

[24] S. Bubin, J. Komasa, M. Stanke, and L. Adamowicz, Isotope shifts of the $1s^22s^2(^1s_0) \rightarrow 1s^22p^2(^1s_0)$ transition in the doubly ionized carbon ion C^{2+}, Phys. Rev. A **81**, 052504 (2010).

[25] S. Bubin, M. Stanke, and L. Adamowicz, Non-Born-Oppenheimer calculations of the BH molecule, J. Chem. Phys. **131**, 044128 (2009).

[26] M. Puchalski, J. Komasa, and K. Pachucki, Explicitly correlated wave function for a boron atom, Phys. Rev. A **92**, 062501 (2015).

[27] K. L. Sharkey, M. Pavanello, S. Bubin, and L. Adamowicz, Algorithm for quantum-mechanical finite-nuclear-mass variational calculations of atoms with two p electrons using all-electron explicitly correlated Gaussian basis functions, Phys. Rev. A **80**, 062510 (2009).

[28] K. L. Sharkey and L. Adamowicz, An algorithm for non-relativistic quantum-mechanical finite-nuclear-mass variational calculations of nitrogen atom in $l = 0$, $m = 0$ states using all-electrons explicitly correlated gaussian basis functions, J. Chem. Phys. **140**, 174112 (2014).

[29] R. D. Poshusta and D. B. Kinghorn, Algebrants in many-electron quantum mechanics: Applications of generalized determinants or matrix functions, Int. J. Quantum Chem. **41**, 15 (1992).

[30] M. Wang, G. Audi, A. Wapstra, F. Kondev, M. MacCormick, X. Xu, and B. Pfeiffer, The AME2012 atomic mass evaluation, Chin. Phys. C **36**, 1603 (2012).

[31] K. L. Sharkey and L. Adamowicz, Exponentially and pre-exponentially correlated Gaussians for atomic quantum calculations, J. Chem. Phys. **134**, 094104 (2011).
[32] M. Hamermesh, *Group Theory and Its Application to Physical Problems* (Addison-Wesley, Reading, MA, 1962).
[33] W. E. Caswell and G. P. Lepage, Effective Lagrangians for bound state problems in QED, QCD, and other field theories, Phys. Lett. B **167**, 437 (1986).
[34] K. Pachucki, Effective Hamiltonian approach to the bound state: Positronium hyperfine structure, Phys. Rev. A **56**, 297 (1997).
[35] H. A. Bethe and E. E. Salpeter, *Quantum Mechanics of One- and Two-Electron Atoms* (Plenum, New York, 1977).
[36] A. I. Akhiezer and V. B. Berestetskii, *Quantum Electrodynamics* (Wiley, New York, 1965).
[37] M. Stanke, S. Bubin, and L. Adamowicz, Lowest ten ^1P Rydberg states of beryllium calculated with all-electron explicitly correlated Gaussian functions, J. Phys. B **52**, 155002 (2019).
[38] I. Hornyák, L. Adamowicz, and S. Bubin, Ground and excited ^1S states of the beryllium atom, Phys. Rev. A **100**, 032504 (2019).
[39] H. Araki, Quantum-electrodynamical corrections to energy-levels of helium, Prog. Theor. Phys. **17**, 619 (1957).
[40] J. Sucher, Energy levels of the two-electron atom to order α^3 Ry; ionization energy of helium, Phys. Rev. **109**, 1010 (1958).
[41] P. K. Kabir and E. E. Salpeter, Radiative corrections to the ground-state energy of the helium atom, Phys. Rev. **108**, 1256 (1957).
[42] Z.-C. Yan and G. W. F. Drake, Relativistic and QED Energies in Lithium, Phys. Rev. Lett. **81**, 774 (1998).
[43] K. Pachucki, Simple derivation of helium Lamb shift, J. Phys. B **31**, 5123 (1998).
[44] S. Bubin and L. Adamowicz, Lowest ^2S Electronic Excitations of the Boron Atom, Phys. Rev. Lett. **118**, 043001 (2017).
[45] K. Pachucki and J. Komasa, Relativistic and QED Corrections for the Beryllium Atom, Phys. Rev. Lett. **92**, 213001 (2004).
[46] K. Pachucki, $\alpha^4 r$ corrections to singlet states of helium, Phys. Rev. A **74**, 022512 (2006).
[47] M. Puchalski, D. Kędziera, and K. Pachucki, Ionization potential for excited S states of the lithium atom, Phys. Rev. A **82**, 062509 (2010).
[48] M. Puchalski, J. Komasa, and K. Pachucki, Testing quantum electrodynamics in the lowest singlet states of the beryllium atom, Phys. Rev. A **87**, 030502(R) (2013).
[49] J. Hiller, J. Sucher, and G. Feinberg, New techniques for evaluating parity-conserving and parity-violating contact interactions, Phys. Rev. A **18**, 2399 (1978).
[50] R. J. Drachman and J. Sucher, Annihilation in positron-atom collisions: A new approach, Phys. Rev. A **20**, 442 (1979).
[51] R. J. Drachman, Nonrelativistic hyperfine splitting in muonic helium by adiabatic perturbation theory, Phys. Rev. A **22**, 1755 (1980).
[52] J. Hiller, J. Sucher, A. K. Bhatia, and G. Feinberg, Parity-violating electric-dipole transitions in helium, Phys. Rev. A **21**, 1082 (1980).
[53] H. P. Trivedi, Improved matrix elements of $\delta(r_1)$ using approximate wavefunctions, J. Phys. B **13**, 839 (1980).
[54] R. J. Drachman, A new global operator for two-particle delta functions, J. Phys. B **14**, 2733 (1981).
[55] L. M. Wang, C. Li, Z.-C. Yan, and G. W. F. Drake, Isotope shifts and transition frequencies for the S and P states of lithium: Bethe logarithms and second-order relativistic recoil, Phys. Rev. A **95**, 032504 (2017).
[56] M. Puchalski and K. Pachucki, Relativistic, QED, and finite nuclear mass corrections for low-lying states of Li and Be^+, Phys. Rev. A **78**, 052511 (2008).
[57] A. E. Kramida and A. N. Ryabtsev, A critical compilation of energy levels and spectral lines of neutral boron, Phys. Scr. **76**, 544 (2007).